Original Research

Cardiac dysfunction in $HgCl_2$-induced nephrotic syndrome

Mónica Moreira-Rodrigues[1], Tiago Henriques-Coelho[2], Cláudia Moura[2], Francisco Vasques-Nóvoa[2], Benedita Sampaio-Maia[1,3], Manuel Pestana[1,4] and Adelino F Leite-Moreira[2]

[1]Unit of Research and Development of Nephrology; [2]Department of Physiology, Faculty of Medicine; [3]Faculty of Dental Medicine, University of Porto; [4]Department of Nephrology, Hospital S. João, Porto, Portugal

Corresponding author: Adelino F Leite-Moreira, Department of Physiology, Faculty of Medicine of Porto, Al. Prof. Hernâni Monteiro, 4200–319 Porto, Portugal. Email: amoreira@med.up.pt

Abstract

The experimental model of $HgCl_2$ injection is characterized by a systemic autoimmune disease which leads to the development of nephrotic syndrome (NS). NS seems to be accompanied by cardiovascular alterations, since patients with NS present an increased incidence in cardiac disease. The aim of our work was to study the effects of $HgCl_2$-induced NS on myocardial function and morphometry. Normotensive Brown–Norway rats were injected with $HgCl_2$ (1 mg/kg, $HgCl_2$ group; $n = 6$, subcutaneous) or the vehicle (control group; $n = 6$, subcutaneous) on days 0, 2, 4, 7, 9 and 11. The animals were placed in metabolic cages for evaluation of urinary excretion of noradrenaline, sodium, total proteins, albumin and creatinine. Fourteen and 21 days after the first $HgCl_2$ injection, left ventricle (LV) hemodynamics was evaluated through pressure micromanometers in basal and isovolumetric heartbeats. The heart and gastrocnemius muscle weights and tibial length were also examined. In an additional group of animals cardiac dimensions and ejection fraction were assessed by echocardiography and LV apoptosis and fibrosis were studied. $HgCl_2$-injected rats presented proteinuria, albuminuria, hyperlipidemia, anemia, sodium retention and ascites at day 14. These alterations were accompanied by LV hemodynamic changes only in isovolumetric heartbeats. Similarly, on day 21, $HgCl_2$-injected rats presented proteinuria, albuminuria, hyperlipidemia, anemia, but no sodium retention or ascites. These animals presented LV systolic and diastolic dysfunction in both basal and isovolumetric heartbeats, as well as cardiac atrophy, LV fibrosis and an increase in myocyte apoptosis. In conclusion, $HgCl_2$-induced NS is accompanied by LV dysfunction and can be a promising model for studying the link between NS and cardiac disease.

Keywords: $HgCl_2$, nephrotic syndrome, systemic autoimmune disease, heart function, proteinuria, cardiac atrophy, noradrenaline, sodium retention

Experimental Biology and Medicine 2010; **235**: 392–400. DOI: 10.1258/ebm.2009.009147

Introduction

The experimental model of kidney injury induced by subcutaneous injections of $HgCl_2$ is widely used to study nephrotic syndrome (NS).[1–6] Mercury chloride induces a systemic autoimmune disease with production of auto-antibodies to laminin-1 and other auto-antigens. The systemic autoimmune disease results in membranous nephropathy with IgG deposits.[3] Immune complexes damage glomerular structures by attracting inflammatory cells, triggering resident glomerular cells to release vasoactive substances, cytokines and activators of coagulation, and activating the complement system.[7,8] The membranous nephropathy is responsible for the development of a high-range proteinuria, hyperlipidemia and full-blown NS associated with generalized edema and ascites.[1–3,6]

An increasing body of evidence is emerging on the cardiovascular alterations that can accompany NS. There are some reports on patients with NS that present an increased incidence in cardiac pathology.[9–11] Some manifestations of NS, like proteinuria and hyperlipidemia, are associated with an increased risk of cardiac morbidity and mortality.[12,13] Cardiovascular diseases secondary to arteriosclerosis are the main causes of morbidity and mortality in patients with systemic autoimmune diseases like rheumatoid arthritis and systemic lupus erythematous.[14] In addition, protein wasting and systemic inflammatory activation during NS induced by puromycin aminonucleoside contribute to cardiac remodeling and dysfunction in this rat model.[15,16] Therefore, the aim of the present study was to evaluate the effects of NS induced by $HgCl_2$ on left

ventricular function and to study the myocardial response to this syndrome.

Materials and methods

In vivo studies

Animals

All *in vivo* investigations were performed in accordance with the European Directive number 86/609, transposed to the Portuguese Law by DL 129/92 and by Portaria 1005/92. Brown–Norway male rats ($n = 36$; Harlan, Barcelona, Spain), with a body weight of 160 ± 10 g, were kept under controlled environmental conditions (12:12 h light/dark cycle and $22 \pm 2^{\circ}$C room temperature).

Experimental model

The animals received subcutaneous injections of 1 mg/kg body weight of $HgCl_2$ ($HgCl_2$ group; Sigma, St Louis, MO, USA) or the vehicle (control [Ctrl] group; NaCl 0.9%) on days 0, 2, 4, 7, 9 and 11. $HgCl_2$-injected rats were fed *ad libitum* throughout the study with ordinary rat chow (0.19% sodium; Panlab, Barcelona, Spain). In order to control anorexia and sodium intake, the daily intake of rat chow in the Ctrl group was limited to the intake of $HgCl_2$ group.

Metabolic study

The animals were placed in metabolic cages (Tecniplast, Buguggiate-VA, Italy) for the collection of 24 h urine for later biochemical determinations. The vials collecting urine for quantification of catecholamines contained 0.5 mL hydrochloric acid (6 mol/L), to avoid the spontaneous oxidation of the amines and its derivatives.

Hemodynamic studies

Fourteen and 21 days after first injection, animals were anesthetized with pentobarbital sodium (50 mg/kg body weight; intraperitoneal) and ascites volume was measured moistening and weighting an absorbent paper. Afterwards, animals were placed on a heated plate (body temperature 36–38°C) and the trachea was cannulated (Abocath 16 G), for mechanical ventilation (60 cpm; tidal volume of 1 mL/100 g; Harvard Small Animal Ventilator, Model 683) with oxygen-enriched air. The heart was then exposed through a median sternotomy and the pericardium widely opened. The ascending aorta was carefully dissected to allow its occlusion during the experimental protocol. Left ventricular pressures were measured with a 2-Fr high-fidelity micromanometer (SPR-324, Millar Instruments, Houston, TX, USA), inserted through the apex. After complete instrumentation, the animal preparation was allowed to stabilize for 15 min. Afterload elevations were performed by abrupt occlusion of the ascending aorta during diastole. The first heartbeat following constriction (isovolumetric beat; ISO) was compared with the preceding basal heartbeat (basal). These beat-to-beat interventions allow selective afterload elevation without neurohumoral activation, pericardial constraint and preload or long-term load history changes.[17] After each occlusion, the animal was allowed to stabilize for several heartbeats. Hemodynamic recordings were made with ventilation suspended at end-expiration. Parameters were converted on-line to digital data with a sampling frequency of 1000 Hz. Maximum pressure (P_{max}), peak rates of pressure rise (dP/dt_{max}) and fall (dP/dt_{min}) and diastolic dysfunction were measured. Relaxation rate was estimated with the time constant τ by fitting the ISO pressure fall to a mono-exponential function. Afterload-induced diastolic dysfunction was assessed by computing the difference between end-diastolic pressure after and before an ISO cycle, as previously reported.[18,19] At the end of the experiment blood was collected from the heart in tubes containing heparin and lithium/heparin for later determination of biochemical parameters.

Morphometric analysis

The heart, left ventricle (LV) and gastrocnemius muscle were weighted and the tibial length was measured.

Echocardiographic assessment

Fourteen and 21 days after first injection, an additional group of animals were anesthetized with pentobarbital sodium (50 mg/kg body weight; intraperitoneal) and echocardiographic examination was assessed. Echocardiography was carried out using a GE Vivid 7 system (GE VingMed) equipped with a standard phased-array 10 MHz transducer. All echocardiography recordings were made in sinus rhythm, at a sweep speed of 200 mm/s for off-line analysis. From the left parasternal short-axis view, two-dimensional guided M-mode tracings were made just below the mitral valve at the level of the papillary muscles for measurements of the interventricular septum (IVS, mm), left ventricular internal diameter (LVD, mm) and left ventricular posterior wall (LVPW) in diastole and systole. Left ventricular ejection fraction (EF) was calculated by use of the cube method according to the formula: $EF = [(LVDd^3 - LVDs^3)/LVDd^3] \times 100$, and the fractional shortening (FS) was calculated from measurements for the LVD in systole and diastole, applying the formula: $FS\ (\%) = [(LVDd - LVDs)/LVDd] \times 100$. All data were collected by use of a trackball-driven cursor and ultrasound system software. The measured beats were selected on the basis of quality of the recording and presence of a regular cardiac rhythm. For each parameter the mean of three representative cardiac cycles was calculated. The measurements were performed off-line using dedicate software (EchoPAC 7).

In vitro studies

Assay of catecholamines

The quantification of noradrenaline in urine was performed by HPLC with electrochemical detection, as previously described.[20] In our laboratory, the lower limit of detection of noradrenaline ranged from 350 to 1000 fmol.

Plasma and urine ionogram and biochemistry

The quantification of sodium was performed by ion-selective electrodes, total proteins by the biuret reaction and creatinine by the Jaffé method, through Cobas Mira Plus analyzer (ABX Diagnostics, Geneva, Switzerland). Creatinine clearance, sodium balance and fractional

excretion of sodium were calculated as described.[6,21] The quantification of cholesterol was performed by selective inhibition colorimetric assay and the quantification of triglycerides (GPO/PAP method) and urea (urease/GLDH method) were performed by enzymatic colorimetric tests, through Cobas Mira Plus analyzer. The quantification of calcium (OPC method) and phosphorous (phosphomolibdate method) was performed by a photometric method, through Cobas Mira Plus analyzer. The quantification of albumin was performed by a photometric method, through an Olympus analyzer. The number of red blood cells was quantified by RF/DC detection method with hydrodynamic focusing (DC detection) and hemoglobin concentration was quantified by sodium lauryl sulfate-hemoglobin method, through a Sysmex XE-5000.

Morphometric determination of cardiac fibrosis

LV sections from the remote regions were stained with Sirius red stain to distinguish areas of connective tissue. The percentage of red staining, indicative of fibrosis, was measured in 10 fields randomly selected on each section (ImageJ, NIH, USA). The value was expressed as the ratio of Sirius red-stained fibrosis area to total area. All sections were evaluated under blind conditions without prior knowledge of which section belonged to which rat.

Detection of apoptotic cardiomyocytes

To assess the extent of apoptosis the terminal deoxynucleotidyl-transferase-mediated dUTP nick end-labeling (TUNEL) assay was used (CardioTACSTM *in situ* Apoptosis Detection Kit, R&D Systems, Minneapolis, MN, USA). Briefly, after deparaffinization LV slides were immersed in phosphate- buffered saline (PBS) and then permeabilized with proteinase K for 20 min at room temperature. Endogenous peroxidase activity was quenched using 5.0% hydrogen peroxide. Then, specimens were incubated in terminal deoxynucleotidyl transferase (TdT) labeling buffer for five minutes. After that, slides were incubated with a mix containing the TdT and biotinylated nucleotides for one hour at 37°C, blocked with stop buffer and incubated with streptavidin-horseradish peroxidase for 10 min at room temperature. After washing in PBS, the slides were finally developed using TACS Blue Label. Nuclear staining by Nucler Fast Red was performed as counterstaining. TUNEL-positive cardiomyocytes were counted in at least 50 optical fields (400×) of each specimen. The apoptotic rate was expressed as a percentage of apoptotic cells of all cardiomyocytes per field.

Statistics

Results are means ± SE of values for the indicated number of determinations. Statistical analysis used a two-way analysis of variance (ANOVA) to compare differences among groups. The Student–Newman–Keuls test was used for multiple comparisons when significant differences were detected. A $P < 0.05$ was assumed to denote a significant difference. All the P values are presented.

Results

Nephrotic syndrome characterization

As shown in Table 1, $HgCl_2$-injected rats developed NS as early as 14 days after the first injection and showed proteinuria, hypoalbuminemia, hyperlipidemia and anemia. There were no significant differences in creatinine clearance, phosphorous and calcium plasmatic levels among the studied groups (Table 1). Plasma levels of urea nitrogen were only increased on day 14 after $HgCl_2$ injection (Table 1).

The sodium intake throughout the study was similar in both $HgCl_2$-injected and control animals. On day 14, $HgCl_2$-injected rats presented a positive sodium balance with a reduction in the fractional excretion of sodium

Table 1 Characteristics of $HgCl_2$-induced nephrotic syndrome ($HgCl_2$) and control (Ctrl) rats, 14 and 21 days after the first injection

	14 days			21 days		
	Ctrl	$HgCl_2$	*P*	Ctrl	$HgCl_2$	*P*
Ascites (g)	0.6 ± 0.1	1.6 ± 0.2*	0.001	0.6 ± 0.3	0.6 ± 0.1	
Creatinine clearance (mL/min)	1.47 ± 0.20	1.55 ± 0.09		1.86 ± 0.15	1.57 ± 0.26	
Sodium homeostasis						
Na^+ balance (mmol/24 h)	0.04 ± 0.07	0.50 ± 0.05*	3×10^{-4}	0.11 ± 0.09	−1.00 ± 0.49*	0.05
FE_{Na+} (%)	0.33 ± 0.05	0.14 ± 0.02*	0.006	0.30 ± 0.03	0.28 ± 0.01	
Blood/plasma analysis						
Red blood cells (10^{12} cells/L)	8.1 ± 0.1	6.9 ± 0.4*	0.002	8.2 ± 0.1	7.3 ± 0.2*	0.005
Blood hemoglobin (g/dL)	14.1 ± 0.2	11.3 ± 0.7*	0.003	14.4 ± 0.1	12.3 ± 0.6*	0.001
Plasma cholesterol (mg/dL)	57.2 ± 1.2	149.7 ± 26.4*	0.006	63.6 ± 1.1	122.5 ± 0.5*	5×10^{-7}
Plasma triglycerides (mg/dL)	89.0 ± 12.4	217.7 ± 50.8*	0.03	77.0 ± 4.4	264.0 ± 15.0*	2×10^{-6}
Plasma Ca^{2+} (mg/dL)	10.3 ± 0.3	10.6 ± 0.3		10.8 ± 0.3	11.6 ± 0.3	
Plasma phosphorous (mg/dL)	8.5 ± 0.4	8.3 ± 0.2		8.3 ± 0.3	6.6 ± 1.0	
Plasma urea (mg/dL)	28.7 ± 1.4	59.5 ± 5.6*	0.0003	27.2 ± 1.7	33.1 ± 1.6	
Plasma albumin (g/L)	27.1 ± 0.7	17.0 ± 1.5*	0.0001	26.7 ± 0.5	18.4 ± 1.0*	2×10^{-5}
Urine analysis						
Urinary proteins (mg/24 h)	10.7 ± 1.9	233.5 ± 96.6*	0.03	9.0 ± 2.4	291.7 ± 44.3*	8×10^{-5}
Urinary albumin (mg/24 h)	0.15 ± 0.06	1.29 ± 0.54*	0.03	0.12 ± 0.07	32.39 ± 11.05*	0.02

Values are mean ± SE of six experiments per group
FE_{Na+}, fractional excretion of sodium
*Significantly different from values in control rats (Ctrl)

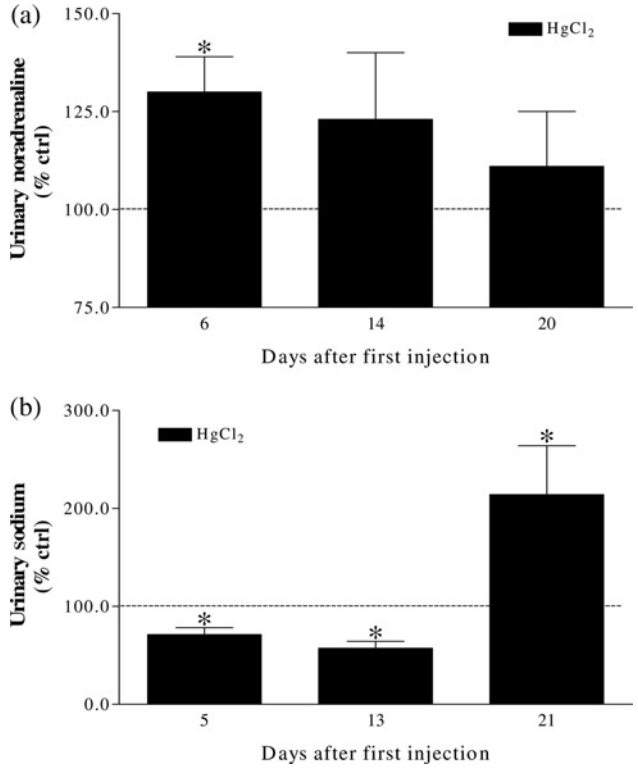

Figure 1 (a) Urinary levels of noradrenaline (nmol/24 h) in $HgCl_2$-induced nephrotic syndrome ($HgCl_2$) expressed as % of control (Ctrl) at different time-points (days 6, 14 and 20). *Significantly different from control rats, $P = 0.02$. (b) Urinary levels of sodium (mmol/mg creatinine) in $HgCl_2$-induced nephrotic syndrome ($HgCl_2$) expressed as % of Ctrl at different time-points (days 5, 13 and 21). *Significantly different from control rats, $P = 0.02$ (day 5), $P = 0.002$ (day 13); $P = 0.05$ (day 21). Bars represent means of six experiments per group and error bars represent SE

and ascites accumulation (Table 1). On day 21, the $HgCl_2$-injected rats presented a negative sodium balance and no ascites accumulation (Table 1). $HgCl_2$-injected rats presented a reduced urinary sodium excretion at 5 and 13 days after first injection and an increased urinary sodium excretion at day 21 as compared with Ctrl rats (Figure 1b). Urinary noradrenaline was increased on day 6 and no differences were detected at days 14 and 20 after first $HgCl_2$ injection (Figure 1).

Morphometric analysis

On day 14, there was an increase in body weight in $HgCl_2$-treated rats. On the contrary, at day 21, $HgCl_2$-treated animals presented body cachexia. The changes observed in body weight were not associated with a decrease in food intake.

No significant differences were observed in LV-weight-to-tibial-length ratio among groups at day 14 (Table 2). On day 21, $HgCl_2$-injected rats presented decreased heart-weight-to-tibial-length and LV-weight-to-tibial-length ratios as compared with Ctrl rats (Table 2). A decrease in gastrocnemius-weight-to-tibial-length ratio was presented in $HgCl_2$ groups at days 14 and 21 (Table 2).

Hemodynamic and echocardiographic evaluation

On day 14, both Ctrl and $HgCl_2$ animals presented similar P_{max}, dP/dt_{max} (Figure 2), dP/dt_{min} and time constant τ (Figure 3) at baseline conditions. These results were further confirmed by echocardiography that showed no differences between groups at day 14 under baseline conditions. On the other hand, there were differences between groups in isovolumetric heartbeats; $HgCl_2$-injected rats presented a significant decrease in P_{max} (Figure 2a) and a slower relaxation rate as showed by an increase in time constant τ (Figure 3b). When we evaluated the difference between the end-diastolic pressure of the isovolumetric heartbeat and the end-diastolic pressure of the baseline heartbeat on day 14, we observed that $HgCl_2$-injected rats had afterload-induced diastolic dysfunction (Figure 4).

On day 21, $HgCl_2$-injected rats presented hemodynamic and echocardiographic signs of cardiac dysfunction even at baseline conditions. $HgCl_2$ group showed systolic failure manifested by a decrease in both P_{max} and dP/dt_{max} (Figure 2). These animals also had a lower $|dP/dt_{min}|$ (Figure 3a). In the echocardiographic assessment, $HgCl_2$-injected rats presented an increase in systolic LVD and a decrease in both fractional shortening and ejection fraction (Table 3). When the LV was submitted to an abrupt increase in afterload (isovolumetric heartbeat) these animals had lower P_{max}, dP/dt_{max} and $|dP/dt_{min}|$, larger τ (Figures 2 and 3) and more pronounced afterload-induced diastolic dysfunction (Figure 4) than control animals.

Cardiac fibrosis and apoptosis

Regarding the cardiac fibrosis, we evaluated the LV interstitial collagen content that was significantly increased in both groups treated with $HgCl_2$ (Figure 5).

Table 2 Morphometric parameters and characterization of left ventricle and skeletal muscle atrophy in $HgCl_2$-induced nephrotic syndrome ($HgCl_2$) and control (Ctrl) rats, 14 and 21 days after the first injection

	14 days			21 days		
	Ctrl	$HgCl_2$	*P*	Ctrl	$HgCl_2$	*P*
Body weight (g)	180 ± 3	190 ± 3*	0.03	197 ± 3	159 ± 3*	4×10^{-6}
Heart weight/tibial length (mg/mm)	162.0 ± 5.8	183.5 ± 6.1*	0.03	165.6 ± 4.0	154.0 ± 3.6*	0.05
LV weight/tibial length (mg/mm)	112.7 ± 3.7	113.3 ± 6.5		117.1 ± 3.1	108.1 ± 3.2*	0.05
Gast. weight/tibial length (mg/mm)	381.4 ± 8.3	311.3 ± 2.6*	1×10^{-5}	387.2 ± 6.3	243.6 ± 8.3*	1×10^{-11}

Values are mean $\pm$ SE per group
LV, left ventricle; Gast., gastrocnemius muscle
*Significantly different from values in control rats (Ctrl)

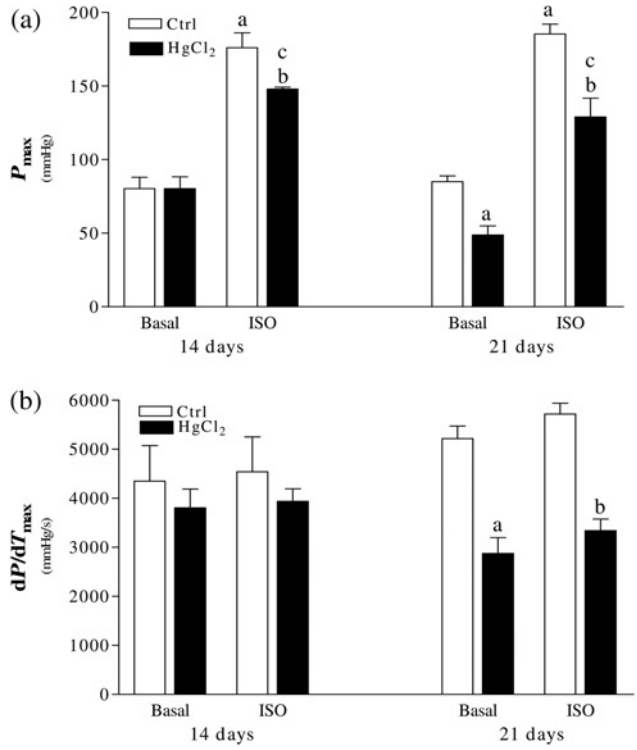

Figure 2 Left ventricular (a) maximum pressure (P_{max}) and (b) peak rate of pressure rise (dP/dt_{max}), at baseline (basal) and in isovolumetric heartbeats (ISO), in $HgCl_2$-induced nephrotic syndrome ($HgCl_2$) and control (Ctrl) rats, 14 and 21 d after the first injection. [a]Significantly different from basal heartbeat in control rats (Ctrl). [b]Significantly different from ISO heartbeat in control rats (Ctrl). [c]Significantly different from basal heartbeat in $HgCl_2$ rats. Bars represent means of six experiments per group and error bars represent SE. (a) Statistical analysis: 14 d: $P = 2 \times 10^{-5}$ (Ctrl ISO versus Ctrl basal); $P = 0.02$ ($HgCl_2$ ISO versus Ctrl ISO); $P = 8 \times 10^{-6}$ ($HgCl_2$ ISO versus $HgCl_2$ basal); 21 d: $P = 1 \times 10^{-7}$ (Ctrl ISO versus Ctrl basal); $P = 6 \times 10^{-4}$ ($HgCl_2$ basal versus Ctrl basal); $P = 0.003$ ($HgCl_2$ ISO versus Ctrl ISO); $P = 0.0002$ ($HgCl_2$ ISO versus $HgCl_2$ basal). (b) Statistical analysis: 21 d: $P = 2 \times 10^{-4}$ ($HgCl_2$ basal versus Ctrl basal); $P = 2 \times 10^{-5}$ ($HgCl_2$ ISO versus Ctrl ISO)

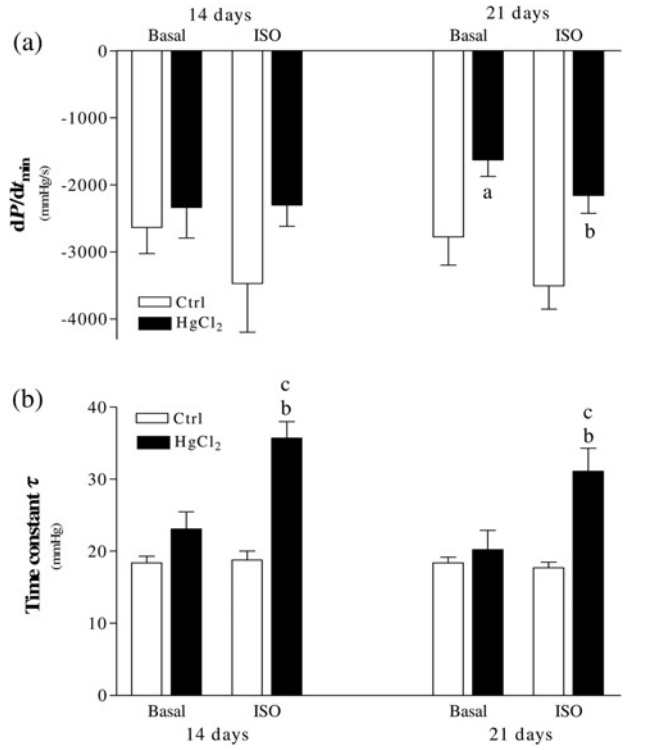

Figure 3 Diastolic hemodynamic parameters. (a) Left ventricular peak rate of pressure fall (dP/dt_{min}) and (b) time constant τ, at baseline (basal) and in isovolumetric heartbeats (ISO), in $HgCl_2$-induced nephrotic syndrome ($HgCl_2$) and control (Ctrl) rats, 14 and 21 d after the first injection. [a]Significantly different from basal heartbeat in control rats (Ctrl). [b]Significantly different from ISO heartbeat in control rats (Ctrl). [c]Significantly different from in basal heartbeat in $HgCl_2$ rats. Bars represent means of six experiments per group and error bars represent SE. (a) Statistical analysis: 21 d: $P = 0.04$ ($HgCl_2$ basal versus Ctrl basal); $P = 0.01$ ($HgCl_2$ ISO versus Ctrl ISO). (b) Statistical analysis: 14 d: $P = 7 \times 10^{-5}$ ($HgCl_2$ ISO versus Ctrl ISO); $P = 0.004$ ($HgCl_2$ ISO versus $HgCl_2$ basal); 21 d: $P = 0.002$ ($HgCl_2$ ISO versus Ctrl ISO); $P = 0.03$ ($HgCl_2$ ISO versus $HgCl_2$ basal)

Apoptosis was only significantly augmented in the LV myocardium of $HgCl_2$-group at 21 d, as compared with controls (Figure 6a). In the representative examples presented in Figure 6b apoptotic cardiomyocytes can be clearly identified at 21 d in $HgCl_2$ group.

Discussion

Mercury chloride acts as an immunotoxic inducing systemic autoimmune disease, which is responsible for the development of NS.[1,3] The glomerulonephritis mediated by immune complexes induced by $HgCl_2$ is a well-established experimental model of NS.[2,3,6] In the present study, we demonstrated for the first time cardiac dysfunction in the experimental model of NS induced by $HgCl_2$. We found that 14 days after the first injection of $HgCl_2$, there is already a severe NS but only subtle changes in cardiac function. However, 21 days after the first $HgCl_2$ injection the animals maintained the NS, presented body cachexia, LV systolic and diastolic dysfunction as well as an increase in cardiomyocyte apoptosis.

Inflammatory activation, which frequently follows malnutrition, has been consistently reported in the NS.[22–25] Disturbances in the growth hormone/insulin-like growth factor 1 (GH/IGF-1) axis have been demonstrated in NS, with increased renal excretion and reduced circulating levels of IGF-1 and IGF-binding proteins.[26] These disturbances might contribute to growth and development

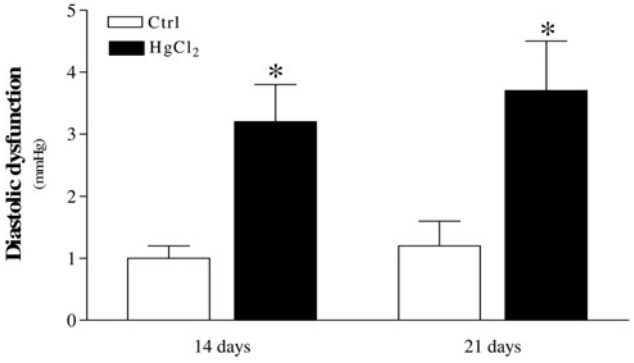

Figure 4 Afterload-induced left ventricular (LV) diastolic dysfunction in $HgCl_2$-induced nephrotic syndrome ($HgCl_2$) and control (Ctrl) rats, 14 and 21 days after the first injection. Bars represent means of six experiments per group and error bars represent SE. *Significantly different from control rats (Ctrl). Statistical analysis: 14 d: $P = 0.006$; 21 d, $P = 0.02$

Table 3 Heart echocardiography assessment in $HgCl_2$-induced nephrotic syndrome ($HgCl_2$) and control (Ctrl) rats, 14 and 21 days after the first injection

	14 days			21 days		
	Ctrl	$HgCl_2$	*P*	Ctrl	$HgCl_2$	*P*
IVSd (mm)	1.52 ± 0.08	1.57 ± 0.07		1.53 ± 0.13	1.55 ± 0.09	
IVSs (mm)	2.54 ± 0.05	2.68 ± 0.08		2.54 ± 0.18	2.53 ± 0.13	
LVDd (mm)	6.50 ± 0.14	6.91 ± 0.16		6.18 ± 0.14	6.19 ± 0.26	
LVDs (mm)	3.18 ± 0.11	3.54 ± 0.16		3.06 ± 0.09	3.49 ± 0.14*	0.03
LVPWd (mm)	1.25 ± 0.04	1.32 ± 0.06		1.33 ± 0.08	1.25 ± 0.04	
LVPWs (mm)	2.19 ± 0.07	2.23 ± 0.09		2.06 ± 0.05	1.90 ± 0.08	
SF (%)	51.01 ± 1.67	48.87 ± 1.67		50.09 ± 1.56	43.55 ± 1.40*	0.01
EF (%)	86.56 ± 1.26	84.72 ± 1.36		85.90 ± 1.25	80.02 ± 1.34*	0.009

Values are mean ± SE per group
IVS, interventricular septum; LVD, left ventricular internal diameter; LVPW, left ventricular posterior wall; d, diastole; s, systole; SF, fractional shortening; EF, ejection fraction
*Significantly different from values in control rats (Ctrl)

retardation described both in experimental models and in children with poorly controlled NS.[27,28] In our study, growth retardation, estimated by tibial length, was not impaired in $HgCl_2$-injected rats, which can be due to the short time span of our study and food ingestion restriction in the Ctrl group. The control of food intake is particularly relevant, given the contribution of anorexia to the malnutrition present in the NS.[29] We found important changes

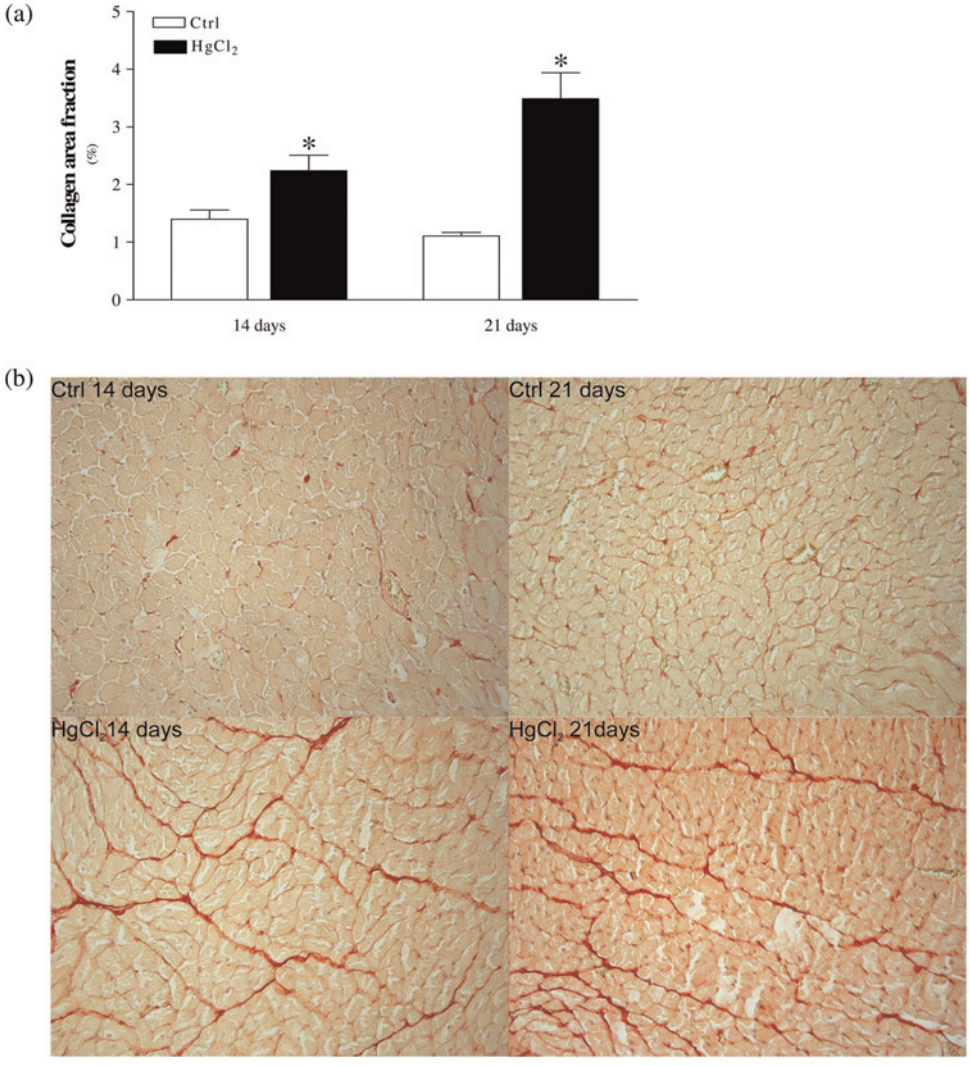

Figure 5 (a) Left ventricular (LV) fibrosis expressed as collagen area fraction and (b) representative examples in $HgCl_2$-induced nephrotic syndrome ($HgCl_2$) and control (Ctrl) rats, 14 and 21 d after the first injection. *Significantly different from control rats (Ctrl). Statistical analysis: 14 days, $P = 0.02$; 21 days: $P = 0.0004$ (A color version of this figure is available in the online journal)

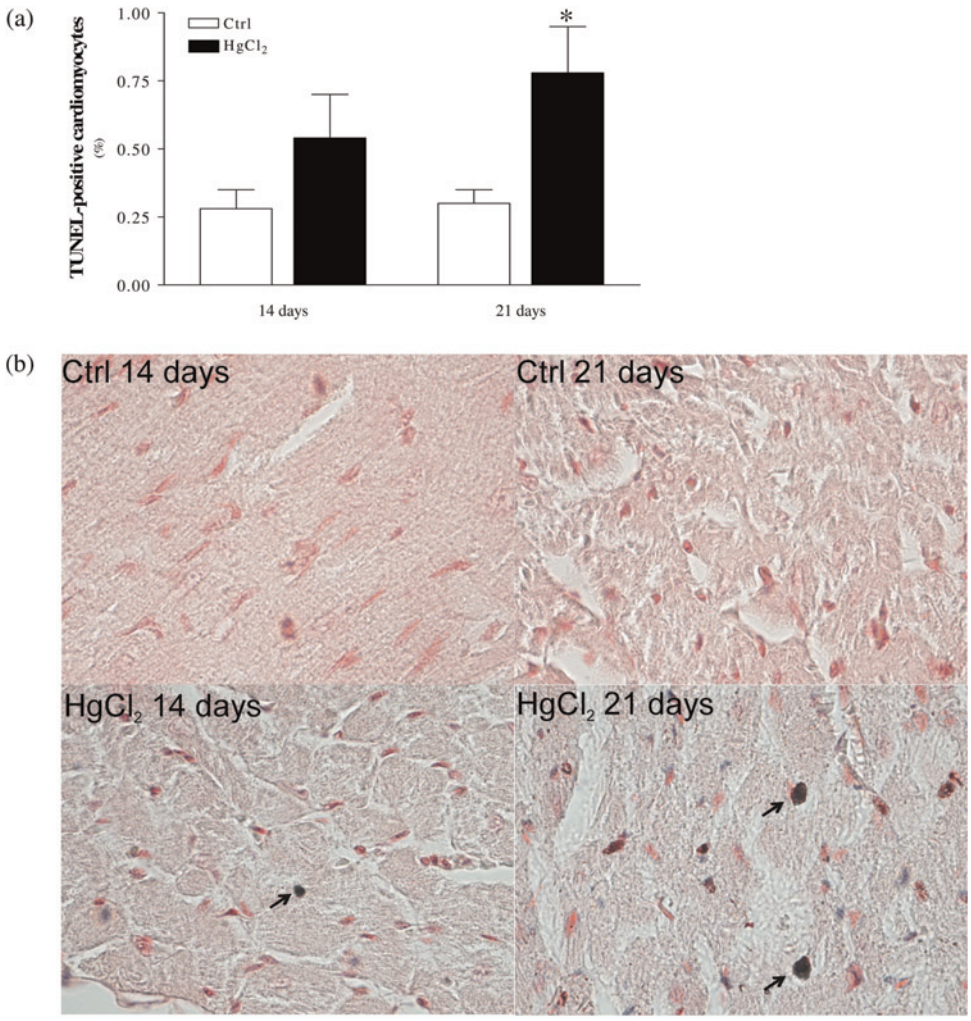

Figure 6 (a) Left ventricular (LV) apoptosis expressed as TUNEL-positive cell percentage and (b) representative examples in $HgCl_2$-induced nephrotic syndrome ($HgCl_2$) and control (Ctrl) rats, 14 and 21 days after the first injection (arrows indicate apoptotic cells). *Significantly different from values in control rats (Ctrl). Statistical analysis: 21 d: $P = 0.02$ (A color version of this figure is available in the online journal)

in body weight of animals injected with $HgCl_2$. The increase in body weight at day 14 could be related to the presence of ascites and the body cachexia reported at day 21 may be related to the worsening of the disease, namely to the cumulative effect of proteinuria.

Our results demonstrate the successful induction of NS and are in accordance with previous studies,[2,3,6] namely proteinuria, hypoalbuminemia, hyperlipidemia and anemia. We observed that sodium retention on day 14 was preceded by an increase in sympathetic activation. Adrenergic system seems to regulate renal tubular sodium transport as demonstrated by other groups.[30,31] They showed that both adrenergic stimulation of renal adrenergic nerves and infusion of low doses of noradrenaline induce an increase in renal tubular sodium reabsorption. In fact, it was suggested that noradrenaline promotes renal sodium reabsorption in proximal convoluted tubules by increasing Na^+, K^+-ATPase activity.[32] On the other hand, activation of the sympathetic system by noradrenaline induces an increase in sodium transporters expression (NHE-3, NBC-1 and BSC-1),[33] suggesting a contribution of sodium retention in pathological diseases with increased sympathetic activity. Therefore, we suggest that the increased sympathetic activity in $HgCl_2$-injected rats may contribute to sodium retention observed until day 14 in this NS model. An increase in sympathetic activity in both animal models and patients with NS and edema was already reported by other authors.[15,34,35] Afterwards, urinary noradrenaline levels normalized and this may contribute to enhanced renal sodium excretion observed on day 21.

Our work presents an extensive characterization of LV function during the development of NS induced by $HgCl_2$. We could identify, as early as 14 days after $HgCl_2$ injection, the presence of LV diastolic dysfunction induced by afterload. We have previously demonstrated that this response to acute afterload elevations can be a precocious sign of cardiac dysfunction, preceding overt heart failure.[36,37] This result was accompanied by other hemodynamic changes present only in isovolumetric hearbeats. These results suggest that even in the absence of reduced glomerular filtration, the mechanisms present during the induction of systemic autoimmune disease, such as ascites, proteinuria, hypoalbuminemia, anemia, hyperlipidemia and increased sympathetic activity, may explain the cardiac intolerance to

afterload. In fact, cardiac edema has been shown to increase myocardial stiffness and induce contractile dysfunction, which has been attributed to increased myocardial expression of aquaporins.[38] In addition, overt proteinuria is an independent predictor of cardiac morbidity and mortality,[12,13] and sympathetic activity alterations may have adverse effects in heart function.[39]

Later in the course of the NS, we observed LV systolic and diastolic dysfunction in both basal and isovolumetric heartbeats 21 days after NS induction by $HgCl_2$. LV dysfunction was accompanied by cardiac and skeletal muscle atrophy, persistent high proteinuria, hypoalbuminemia, anemia and hyperlipidemia. Atrophy of the LV could be related to fibrosis and apoptosis and might contribute to the worsening of cardiac function. These findings are in agreement with previous studies in the passive Heymann nephritis model of NS, providing evidence for impaired muscle protein synthesis.[40] Moreover, in the model of NS induced by puromycin aminonucleoside our group also suggested that LV and skeletal muscle atrophy could contribute to cardiac remodeling and dysfunction.[15] We cannot exclude the potential contribution of $HgCl_2$ autoimmune effects to the cardiac alterations observed in this model of NS.

In conclusion, $HgCl_2$-induced NS is accompanied by ascites, proteinuria, hyperlipidemia and slight hemodynamic changes only 14 days after $HgCl_2$ injection. In the later course of the disease, these alterations are accompanied by LV systolic and diastolic dysfunction, cardiac atrophy and myocyte apoptosis. These findings may contribute to a better characterization of cardiac function in the NS model induced by $HgCl_2$ and might be a promising model for studying the link between NS and cardiac disease.

ACKNOWLEDGEMENTS

This study was supported by Grant PIC/IC/83029/2007 and PTDC/SAU-FCF/65793/2006 from Fundação para a Ciência e Tecnologia/FEDER. M Moreira-Rodrigues was supported by Grant SFRH/BD/18869/2004 and B Sampaio-Maia was supported by the fellowship SFRH/BPD/21782/2005 from Fundação para a Ciência e Tecnologia/FEDER.

REFERENCES

1 Bigazzi PE. Metals and kidney autoimmunity. *Environ Health Perspect* 1999;**107**:753–65
2 Deschenes G, Doucet A. Collecting duct (Na+/K+)-ATPase activity is correlated with urinary sodium excretion in rat nephrotic syndromes. *J Am Soc Nephrol* 2000;**11**:604–15
3 Druet P, Druet E, Potdevin F, Sapin C. Immune type glomerulonephritis induced by $HgCl_2$ in the Brown–Norway rat. *Ann Immunol (Paris)* 1978;**129 C**:777–92
4 Kanfer A. Coagulation factors in nephrotic syndrome. *Am J Nephrol* 1990;**10** (Suppl. 1):63–8
5 Michaud A, Sapin C, Leca G, Aiach M, Druet P. Involvement of hemostasis during an autoimmune glomerulonephritis induced by mercuric chloride in Brown–Norway rats. *Thromb Res* 1984;**33**:77–88
6 Sampaio-Maia B, Moreira-Rodrigues M, Serrao P, Pestana M. Blunted renal dopaminergic system activity in $HgCl_2$-induced membranous nephropathy. *Life Sci* 2006;**78**:1246–55
7 Nangaku M, Couser WG. Mechanisms of immune-deposit formation and the mediation of immune renal injury. *Clin Exp Nephrol* 2005;**9**:183–91
8 Suzuki K, Kanabayashi T, Nakayama H, Doi K. Kinetics of chemokines and their receptors in mercuric chloride-induced tubulointerstitial lesions in Brown–Norway rats. *Exp Mol Pathol* 2003;**75**:58–67
9 Adedoyin O, Frank R, Vento S, Vergara M, Gauthier B, Trachtman H. Cardiac disease in children with primary glomerular disorders-role of focal segmental glomerulosclerosis. *Pediatr Nephrol (Berlin, Germany)* 2004;**19**:408–12
10 Ordonez JD, Hiatt RA, Killebrew EJ, Fireman BH. The increased risk of coronary heart disease associated with nephrotic syndrome. *Kidney Int* 1993;**44**:638–42
11 Watts GF, Herrmann S, Dogra GK, Playford DA, Best JD, Thomas MA, Irish A. Vascular function of the peripheral circulation in patients with nephrosis. *Kidney Int* 2001;**60**:182–9
12 Ritz E, Dikow R, Ruilope LM. Renal dysfunction as a cardiovascular risk factor. *Curr Hypertens Rep* 2002;**4**:365–8
13 Segura J, Campo C, Ruilope LM. Proteinuria: an underappreciated risk factor in cardiovascular disease. *Curr Cardiol Rep* 2002;**4**:458–62
14 Avalos I, Rho YH, Chung CP, Stein CM. Atherosclerosis in rheumatoid arthritis and systemic lupus erythematosus. *Clin Exp Rheumatol* 2008;**26**:S5–13
15 Moreira-Rodrigues M, Roncon-Albuquerque R Jr, Henriques-Coelho T, Lourenco AP, Sampaio-Maia B, Santos J, Pestana M, Leite-Moreira AF. Cardiac remodeling and dysfunction in nephrotic syndrome. *Kidney Int* 2007;**71**:1240–48
16 van der Vijgh WJ, Van Velzen D, Van der Poort JS, Schluper HM, Mross K, Feijen J, Pinedo HM. Morphometric study of myocardial changes during puromycin aminonucleoside induced nephropathy in rats. *Anticancer Res* 1987;**7**:1111–5
17 Gillebert TC, Leite-Moreira AF, De Hert SG. Load dependent diastolic dysfunction in heart failure. *Heart Failure Rev* 2000;**5**:345–55
18 Leite-Moreira AF, Correia-Pinto J. Load as an acute determinant of end-diastolic pressure–volume relation. *Am J Physiol Heart Circ Physiol* 2001;**280**:H51–9
19 Leite-Moreira AF, Correia-Pinto J, Gillebert TC. Afterload induced changes in myocardial relaxation: a mechanism for diastolic dysfunction. *Cardiovasc Res* 1999;**43**:344–53
20 Soares-da-Silva P, Fernandes MH, Pestana M. Studies on the role of sodium on the synthesis of dopamine in the rat kidney. *J Pharmacol Exp Therapeut* 1993;**264**:406–14
21 Sampaio-Maia B, Serrao P, Guimaraes JT, Vieira-Coelho MA, Pestana M. Renal dopaminergic system activity in the rat remnant kidney. *Nephron* 2005;**99**:e46–55
22 Bustos C, Gonzalez E, Muley R, Alonso JL, Egido J. Increase of tumour necrosis factor alpha synthesis and gene expression in peripheral blood mononuclear cells of children with idiopathic nephrotic syndrome. *Eur J Clin Investig* 1994;**24**:799–805
23 Gomez-Chiarri M, Ortiz A, Lerma JL, Lopez-Armada MJ, Mampaso F, Gonzalez E, Egido J. Involvement of tumor necrosis factor and platelet-activating factor in the pathogenesis of experimental nephrosis in rats. *Lab Investig J Tech Methods Pathol* 1994;**70**:449–59
24 Raveh D, Shemesh O, Ashkenazi YJ, Winkler R, Barak V. Tumor necrosis factor-alpha blocking agent as a treatment for nephrotic syndrome. *Pediatric nephrology (Berlin, Germany)* 2004;**19**:1281–4
25 Suranyi MG, Guasch A, Hall BM, Myers BD. Elevated levels of tumor necrosis factor-alpha in the nephrotic syndrome in humans. *Am J Kidney Dis* 1993;**21**:251–9
26 Haffner D, Tonshoff B, Blum WF, Vickers M, Siebler T, Cronin MJ, Baxter RC, Mehls O. Insulin-like growth factors (IGFs) and IGF binding proteins, serum acid-labile subunit and growth hormone binding protein in nephrotic children. *Kidney Int* 1997;**52**:802–10
27 Thabet MA, Challa A, Chan W, Liu F, Hintz RL, Chan JC. Insulin-like growth factor and growth hormone receptor in nephrotic rats. *Am J Physiol* 1994;**266**:E102–6
28 Zhou X, Loke KY, Pillai CC, How HK, Yap HK, Lee KO. IGFs and IGF-binding proteins in short children with steroid-dependent nephrotic syndrome on chronic glucocorticoids: changes with 1 year exogenous GH. *Eur J Endocrinol/Eur Fed Endocrine Soc* 2001;**144**:237–43
29 Dong F, Ren J. Insulin-like growth factors (IGFs) and IGF-binding proteins in nephrotic syndrome children on glucocorticoid. *Pharmacol Res* 2003;**48**:319–23
30 DiBona GF. Neural control of renal tubular sodium reabsorption of the dog. *Fed Proc* 1978;**37**:1214–7

31 Gullner HG. The role of the adrenergic nervous system in sodium and water excretion. *Klinische Wochenschrift* 1983;**61**:1063–6
32 Beach RE, Schwab SJ, Brazy PC, Dennis VW. Norepinephrine increases Na+-K+-ATPase and solute transport in rabbit proximal tubules. *Am J Physiol* 1987;**252**:F215–20
33 Sonalker PA, Tofovic SP, Bastacky SI, Jackson EK. Chronic noradrenaline increases renal expression of NHE-3, NBC-1, BSC-1 and aquaporin-2. *Clin Exp Pharmacol Physiol* 2008;**35**:594–600
34 DiBona GF, Sawin LL, Jones SY. Characteristics of renal sympathetic nerve activity in sodium-retaining disorders. *Am J Physiol* 1996;**271**:R295–302
35 Rahman SN, Abraham WT, Van Putten VJ, Hasbargen JA, Schrier RW. Increased norepinephrine secretion in patients with the nephrotic syndrome and normal glomerular filtration rates: evidence for primary sympathetic activation. *Am J Nephrol* 1993;**13**:266–70
36 Correia-Pinto J, Henriques-Coelho T, Roncon-Albuquerque R Jr, Lourenco AP, Melo-Rocha G, Vasques-Novoa F, Gillebert TC, Leite-Moreira AF. Time course and mechanisms of left ventricular systolic and diastolic dysfunction in monocrotaline-induced pulmonary hypertension. *Basic Res Cardiol* 2009;**104**:535–45
37 Lourenco AP, Roncon-Albuquerque R Jr, Bras-Silva C, Faria B, Wieland J, Henriques-Coelho T, Correia-Pinto J, Leite-Moreira AF. Myocardial dysfunction and neurohumoral activation without remodeling in left ventricle of monocrotaline-induced pulmonary hypertensive rats. *Am J Physiol Heart Circ Physiol* 2006;**291**:H1587–94
38 Egan JR, Butler TL, Au CG, Tan YM, North KN, Winlaw DS. Myocardial water handling and the role of aquaporins. *Biochim Biophys Acta* 2006;**1758**:1043–52
39 Lee CS, Tkacs NC. Current concepts of neurohormonal activation in heart failure: mediators and mechanisms. *AACN Adv Crit Care* 2008;**19**:364–85; quiz 386–7
40 Kaysen GA, Carstensen A, Martin VI. Muscle protein synthesis is impaired in nephrotic rats. *Miner Electrolyte Metab* 1992;**18**:228–32

(Received April 30, 2009, Accepted October 26, 2009)